Plasma observations during the June 7, 2021 Ganymede flyby from the Jovian Auroral Distributions Experiment (JADE) on Juno

F. Allegrini[1,2], F. Bagenal[3], R. W. Ebert[1,2], P. Louarn[4], D. J. McComas[5], J. R. Szalay[5], P. Valek[1], R. Wilson[3], S. J. Bolton[1], J. E. P. Connerney[6,7], G. Clark[8], S. Duling[9], W. S. Kurth[10], B. Mauk[8], J. Saur[9], J. H. Waite[1,2]

[1]Southwest Research Institute, San Antonio, Texas, USA

[2]Department of Physics and Astronomy, University of Texas at San Antonio, San Antonio, Texas, USA

[3] Laboratory for Atmospheric and Space Physics, University of Colorado Boulder, Boulder, Colorado, USA.

[4] Institut de Recherche en Astrophysique et Planétologie (IRAP), Toulouse, France.

[5] Department of Astrophysical Sciences, Princeton University, Princeton, New Jersey, USA.

[6] Space Research Corporation, Annapolis, Maryland, USA.

[7] NASA Goddard Space Flight Center, Greenbelt, Maryland, USA.

[8] The Johns Hopkins University Applied Physics Laboratory, Laurel, Maryland, USA.

[9] Institute of Geophysics and Meteorology, University of Cologne, Cologne, Germany.

[10] Department of Physics and Astronomy, University of Iowa, Iowa City, Iowa, USA.

Corresponding author: Frédéric Allegrini (fallegrini@swri.edu)

Key Points:

The plasma observations show that Juno crossed into the open field line region, but do not support crossing into a closed field line region

The ion composition near Ganymede is very different from the local plasma disk environment

H_2^+ and H_3^+ ions were detected inside Ganymede's magnetopause and outside in the wake region

Plain Language Summary

On June 7, 2021 the Juno mission came as close as 1046 km from the surface of Ganymede, the largest moon in the solar system. Similar close encounters were previously made by the Galileo mission, from which we learned much of the interaction of the moon, with its own intrinsic magnetic field, and Jupiter's magnetosphere. In this paper, we present an overview of the plasma observations, i.e. ions and electrons in the lower part of the energy spectrum, made by the Jovian Auroral Distributions Experiment (JADE). We find that the ion composition near Ganymede is very different than that from Jupiter's magnetosphere. Near Ganymede, the plasma composition is dominated by molecules and ions that originate from water in the atmosphere or the surface. One surprising observation is the presence of the molecular ion H_3^+ inside Ganymede's magnetosphere and in a region just outside and downstream, that we call the wake. H_3^+ was not included in various models of Ganymede's atmosphere.

Abstract

We report on plasma observations from Juno/JADE during the Ganymede flyby on June 7th, 2021. Juno approached Ganymede from southern latitudes, passed through the wake region, then through its magnetosphere to closest approach (1046 km from the surface) on the night side, and then back into Jupiter's plasma disk. We describe general plasma properties in the regions explored along the trajectory. We infer that Juno traversed a region of open field lines where one end intercepts Ganymede and the other Jupiter. The observations do not support Juno crossing into the closed field line region. The ion composition near Ganymede is very different than that of the nearby plasma environment. H_2^+ and H_3^+ ions were detected near Ganymede and in the wake region. Low energy (~0.1 to 1 keV) electrons are enhanced just outside the magnetopause, in the wake (inbound trajectory) and in the magnetopause boundary layer (outbound trajectory).

1 Introduction

Most of what is known from the interaction of Ganymede with Jupiter's magnetosphere originates from six Galileo close flybys (ranging from 264.4 km to 3104.9 km in altitude) (e.g., Kivelson et al. 2022).

Approaching its 34th perijove, Juno came as close as 1046 km from Ganymede's surface (sub-spacecraft latitude of 23.6° N) on June 7th, 2021 (Hansen et al. this issue). Juno approached Ganymede from southern latitudes, passed through a part of the wake region that was unexplored by previous missions, through its magnetosphere to closest approach on the night side, then to the dayside, and went back into the plasma disk towards Jupiter. Highlights of the flyby from Juno's suite of instruments are reported in this issue.

In this paper, we summarize plasma observations made by the Jovian Auroral Distributions Experiment (McComas et al. 2017). JADE consists of two electron (JADE-E) and one ion (JADE-I) sensors. JADE-E are top-hat analyzers measuring 0.032 to 32 keV electron distributions at 1 second time resolution. JADE-I has a top-hat analyzer and a time-of-flight (TOF) section to determine ion energy-per-charge (E/q) and mass-per-charge (m/q) from ~0.013 to 46 keV/q at 2 second time resolution. The details of the ion observations are given in Valek et al. (this issue). Evidence for magnetic reconnection near the upstream magnetopause is given in Ebert et al. (this issue) and Romanelli et al. (this issue).

The magnetic field data from the MAG experiment (Connerney et al. 2017) provides context to the plasma observations. Details of the magnetic field from this flyby can be found in Weber et al. and Romanelli et al. in this issue.

JADE's energy range slightly overlaps with the energetic particle instrument JEDI (Mauk et al. 2017). The JEDI ion and electron observations overview is given in Clark et al. (this issue).

2 Flyby geometry and overview

Figure 1 shows Juno's trajectory in the Ganymede-Phi-Orbital (GPhiO) reference frame, where +z aligns with Jupiter's rotation axis, +y is along the Ganymede-Jupiter vector, and +x completes the right-handed Cartesian frame. On each side of the track, we show color-coded ion count rates according to their speed (> or < 80 km/s) in the spacecraft frame. Note that the value of 80 km/s is well below the relative velocity from the plasma disk at Ganymede (~140±20 km/s; Kivelson et al. 2022) and above hydrogen ion outflow bulk speed of ~70 km/s in the polar cap (Frank et al. 1997) and the spacecraft ram speed of ~18 km/s (Hansen et al. this issue). The color-coded rate tracks clearly show that the slower ions dominate near closest approach to Ganymede. The regions labelled "Jupiter's plasma disk" correspond to regions where both ends of the field lines intercept Jupiter's atmosphere. The region labelled "Ganymede's magnetosphere" corresponds to a region of open magnetic field lines where one end connects to Ganymede while the other connects to Jupiter. As we will see below, the JADE data does not show clear signs that Juno has entered the closed field line region, where both ends connect to Ganymede. The region labelled "wake" has a similar ion composition to the plasma disk composition, but has different plasma properties.

3 Ion and electron overview

Figure 2 presents plasma observations from JADE (panels a-h) and magnetic field data from MAG. The vertical dashed lines indicate boundaries (A through E) between regions with different ion and/or electron properties. We defined these boundaries based on changes in the plasma distributions and/or the magnetic field. Table 1 gives the boundary crossing times and brief summaries of the plasma observations. The vertical line labelled "X" is the closest approach to Ganymede (16:56:07 UT). Figure 2 contains detailed information that we summarize below, but we start here with a quick description of the data. The top four panels (a-d) show ion observations. Panel (a) is the energy-time spectrogram of ion counts/s, panel (b) is the same for heavy ions ($m/q \geq 8$), and panel (c) is for light ions ($m/q = 1$). Panel (d) shows the proton (>0.5 keV) pitch angle-time spectrogram. For electrons, panel (e) is the energy-time spectrogram, panel (f) is the pitch angle-time spectrogram, panel (g) is partial electron density, and panel (h) is the electron energy flux in two different pitch angle ranges indicated on the right (0° is towards and 180° is away from Ganymede between C and D). Panel (i) shows the magnetic field strength and its components in the GPhiO reference frame. Juno's latitude, longitude, and altitude with respect to Ganymede are labelled at the bottom of the figure. The electron density shown in panel (g) is called "partial" because JADE measures the fraction of the distribution that is within its energy range. The black symbols are within a factor of about two of the total electron density (see Allegrini et al. 2021). The symbols in gray are lower limits because a significant part of the electron distribution is below JADE-E's energy range. The Waves instrument determines the

total electron density between boundaries C and D and in the plasma disk (Kurth et al. this issue).

Before boundary A – Plasma disk

Juno is in Jupiter's plasma disk at ≥5 Ganymede radii (1 R_G=2631.2 km) at southern Ganymede-centric latitude of −7°. The ion composition is dominated by heavy ions (Kim et al. 2020b). Further details on ion composition are in Table 1, Figure 3, and Section 4. Electron intensities are slightly depleted around 90° pitch angle, becoming more pronounced approaching boundary A. Similar pitch angle distributions (and depletion at 90°) are observed at higher energies (Clark et al. this issue). Ion and electron densities are given in Table 1.

Between A and B

There is no significant change in the ion distributions or composition, but the magnetic field starts to rotate. Right after A the intensities of the ≲1 keV field-aligned electrons increase by up to a factor of ~3.5. The electron flux near 90° pitch angle is increasingly more depleted. Thus, between A and B the plasma conditions look similar to Jupiter's plasma disk (before A), but the influence of Ganymede's magnetosphere starts to increase.

Between B and C – Wake

There are four notable differences compared with plasma disk conditions. First, the heavy ion (panels (a-b)) and the electrons (panel (e)) are heated (broader distributions in energy). Second, the protons are mostly field-aligned near pitch angle 180° (panel (d)). Third, the magnetic field shows small, rapid variations (Weber et al. this issue), and the rotation of the field continues (Weber et al. this issue). Fourth, in addition to the nominal plasma disk composition, JADE also measured ions at m/q=3 (see details in Figure S1 in the Supplemental Information and Section 6).

With the exception of the presence of ions at m/q=3, the ion composition (Figure 2) is very similar to the plasma disk which suggests that this region is connected to Jupiter's magnetosphere. The partial electron density is slightly higher than before A (Table 1).

We call this region the wake, which is the structure downstream of an obstacle – in our case Ganymede's magnetosphere – affected by the flow past it.

Between C and D – Ganymede's magnetosphere, open field line region

The transition at boundary C shows substantial changes in both the ion and electron distributions, but no discontinuity in the magnetic field. Both ion energy and composition change. There are distinct ion populations between C and D (see Section 4 and Table 1). The presence of m/q=2 and 3 (likely from H_2^+ and H_3^+) and heavier ions at m/q=16 and 32 are indicators that these ions are likely water byproducts from Ganymede's atmosphere (Roth et al., 2021). Boundary C is likely the magnetopause. Although less intense, ion distributions and composition similar to the

plasma disk are still visible in panels (a-c), which is evidence that this region still connects to Jupiter's magnetosphere.

The >0.5 keV protons are largely precipitating (pitch angle near 0°) and do not mirror back (empty loss cone near 180°). This indicates that Juno is likely in a region of open field lines (one end connected to Ganymede and the other to Jupiter) and these ion observations provide important information on Ganymede's magnetic topology via loss cone size determination.

From 16:50:43 to 16:50:51, JADE measured beams of heavy ($m/q \geq 8$) and light ($m/q=1$) ions with a very narrow peak in energy (see Figure S2 in the Supplemental Information). Simultaneously, MAG recorded perturbations in the magnetic field. The intensity of the heavy ions peaked at ~150 eV at 16:50:43 and increased up to ~300 eV at 16:50:51. In Figure S2 panel (a), the higher energy beam is from the heavy ions and the lower energy beam is from the light ions. The light ions energy distribution is clearly broader than that of the heavy ions. It is not clear what accelerated these ions and why the energy distribution for the light ions was broader than that of the heavy ions.

The electrons also show changes in both energy and pitch angle in this region. The integral intensity decreases by a factor of ~5 from prior to boundary C. The electron pitch angle coverage is partial until ~16:54:36, but the signs of a loss cone near 180° are visible from ~16:53:30. The conjugate loss cone toward Ganymede near 0° does not seem depleted, indicating a precipitation of Jovian magnetospheric electrons in this energy range to Ganymede's polar regions. See Figure 4 and Section 5 for details.

The (0.032-32 keV) electron energy flux (panel (h)) increases from ~16:54:30 to 17:00:37 (boundary D). The energy flux from electrons with pitch angles from 0 to 45° (red) is higher than that with pitch angles from 135° to 180° (blue), which is a direct consequence of the partially depleted loss cone near 180°. The electrons with pitch angles near 0° (180°) move towards (away from) Ganymede. The depleted loss cone near 180° is another indicator that the field line connects to Ganymede.

<u>Between D and E – Magnetopause boundary layer</u>

The ion and electron properties are similar to those of region A–B, with the exception of the electron pitch angle distributions. There is an enhancement in the intensities near 90° pitch angle and no sign of the depletion (also near 90°) that was seen in the region A-B. The magnetic field rotates back to its orientation in the plasma disk. This region is likely the magnetopause, or magnetopause boundary layer (Ebert et al., this issue), consistent with model predictions (Duling et al. and Romanelli et al., this issue).

The electron energy flux peaks (~10 mW/m^2) right before E and is at a level to excite Ganymede's upstream aurora (Saur et al. this issue). From the current model predictions from Duling et al. (this issue), Juno came as close as 0.13 R_G from the closed field line region right before the magnetopause. Their parameter study reveals that the extent of the closed field line boundary is dynamic in this region and, thus, it is possible that these electrons could be exciting

Ganymede's aurora (Greathouse et al. this issue). However, it would only contribute to emissions near the open-closed field line boundary and not to those that extend to lower latitudes.

There is also evidence for magnetic reconnection in this region (Ebert et al. and Romanelli et al. this issue).

After boundary E – Plasma disk

The region after boundary E is very similar to before A with the notable difference that the electrons with pitch angles around 90° are not depleted.

4 Ion composition

Figure 3 shows ion composition with two sets of plots: panels (a-b) for plasma disk (before boundary A) and panels (c-d) near Ganymede (C–D). Each set comprises an energy-time spectrogram on the top and the average ion counts/s displayed in E/q versus m/q on the bottom.

Panel (b) shows typical ion composition in Jupiter's plasma disk (Kim et al. 2020b). The presence and abundance of H_2^+ is consistent with a population of radially transported pickup ions from Europa's neutral H_2 toroidal cloud (Szalay et al. 2022).

The tilted lines represent a constant speed (80 km/s in black, 80±18 km/s in grey) in the spacecraft reference frame and guides the eye to highlight the clear separation between slow and fast ions. For comparison, the ram speed is ~18 km/s (Hansen et al. this issue) and the relative plasma disk speed is ~140±20 km/s (Kivelson et al. 2022). A detailed analysis of the ion flow direction, velocity distribution, and density profiles in the region C–D is given in Valek et al. (this issue).

Figure 3d shows the ion composition near Ganymede. While the composition above the tilted line is reminiscent of Jupiter's plasma disk from Figure 3b, the highest rates come from below the line. The main peaks are at m/q=1, 2, 3, 16, and 32 which we postulate are H^+, H_2^+, H_3^+, O^+, and O_2^+. A more detailed analysis (similar to that in Kim et al. 2020a) of the low speed ion composition at m/q~16 is necessary since water group ions (H_2O^+ and OH^+) are currently not resolved in the JADE-I data analysis. Nevertheless, the fact that H_2^+ and H_3^+ ions are present is an indicator that the composition is likely dominated by water vapor components of its atmosphere (Roth et al. 2021).

5 Electron distributions

Figure 4 highlights some key features in the electron distributions. Panels (a, b) are in the same format as Figure 2(e, f). Panels (c-g) are electron intensities as a function of energy for three pitch angle ranges. Panels (h-l) are electron intensities as a function of pitch angle for eight energy ranges.

Before boundary A (panels (c, h)), the electron distributions represent the plasma disk conditions in the vicinity of Ganymede. The low energy ($\lesssim$5 keV) pitch angle distributions are slightly field-aligned, whereas the high energy ($\gtrsim$10 keV) ones are more pancake-like.

Between B and C (panel (e)), there is a strong enhancement of intensities for 0.1 to 1 keV electrons, with a peak near ~400 eV. The pitch angle coverage from JADE is partial in this interval and in the first half of the next interval (C-D).

Between C and D (panels (f), (j), and (k)), the intensities drop compared to plasma disk intensities by as much as a factor of ~3 at 0.032 keV and more than an order of magnitude at 32 keV. While the intensities of the low energy electrons ($\lesssim$ 200 eV) do not vary much during this interval, the intensities at 32 keV gradually decrease until they reach a minimum (~10^5 cm^{-2} s^{-1} sr^{-1} keV^{-1}) between 16:53:30 and 16:55:00 (i.e., ~1 minute before closest approach) and then gradually increase (to ~10^6 cm^{-2} s^{-1} sr^{-1} keV^{-1}) until boundary D.

One notable feature indicated by an arrow in panel (f) is a persistent "bump" (around 1 - 2 keV). This "bump" is observed from ~16:52 to ~17:00 (see e.g., Figure S3 in the Supplemental Information). The enhancement is a factor of ~2 higher than an interpolated spectrum between the lower and higher parts of the spectrum. Below the bump, the intensities are steady until ~16:56 (near closest approach), but then increase by a factor of ~2 just below ~1 keV. It seems that the "bump" is caused by field-aligned electrons, but given that the pitch angle coverage is incomplete until ~16:54:36, it is difficult to say for sure. It is not clear what accelerates these electrons (near the bump and just below it). The spectrum is softer near closest approach and harder near the boundaries of this region.

Panels (g, l) characterize the electron distributions near the peak of the energy flux. At that time, the intensity of the field-aligned electrons is enhanced from ~0.032 to ~3keV, with a peak near ~0.4 keV. Electrons below ~3 keV are field-aligned. Notably, there is also an intensity enhancement near 90° pitch angle for energies between ~0.5 and ~6 keV.

The region between D and E is very short, and while it looks like a transition between the open field lines region to Jupiter's magnetosphere, the plasma properties are very similar to regions A-B and B-C. One exception is in the electron pitch angle distributions where the ~0.5 to 6 keV electrons show an enhancement near pitch angle 90°.

6 Discussion

These observations can inform us on the magnetic topology. Focusing on the region C-D (i.e., near Ganymede), they tell us the following:
1) Ion composition is substantially different compared to outside this region. However, the composition of the fast ions is reminiscent of Jupiter's plasma disk, though with reduced intensities.
2) Protons above 0.5 keV precipitate towards Ganymede (pitch angles near 0° in Fig. 2d) and do not mirror back (empty loss cone at pitch angle near 180°).
3) Below ~10 keV, the precipitating electron loss cone is full, while the upward loss cone is depleted (Figs. 2f, 4j, and 4k).

These combined observations suggest that, between boundaries C and D, Juno was in a region of open field lines, with one end connected to Ganymede and the other to Jupiter. Outside of this region (i.e., before C and after D), Juno was in a region where both ends of the magnetic field lines were connected to Jupiter. Thus, boundaries C and D are the magnetopause. We do not see any obvious sign of Juno crossing into Ganymede's closed field line region.

The ≳10 keV electron pitch angle distributions show a depleted downward loss cone (Fig. 4j and also Clark et al. this issue). It could be interpreted as a region of closed field lines. Similar electron pitch angle distributions were measured by Galileo during the G2 flyby over the polar regions as reported by Frank et al. (1997) and Williams et al. (1997). Frank et al. (1997) proposed two possible scenarios, both involving flux tubes that were emptied by Ganymede. For high energy (≳10 keV) electrons, the bounce time to Jupiter and back is shorter than the convection time of a flux tube across Ganymede. Therefore, we would expect flux tubes from high energy electrons to be depleted near 0 and 180° pitch angles, while flux tubes of low energy electrons would only be depleted near 180°.

In the wake region (B-C), JADE measured ions at m/q=3 (see Supplemental Information Figure S1). We assume that these ions are H_3^+, which implies that either they leaked out of Ganymede's magnetosphere or they were created in the wake region where H_2^+ is also observed. Another interesting observation is that H_2^+ and H_3^+ in B-C have significantly higher energies than in C-D. Understanding the origin and the energization of H_3^+ in the wake region deserves further attention.

7 Conclusion

Juno traversed different regions of the interaction between Jupiter's plasma disk and Ganymede's magnetosphere. We briefly described the plasma properties in these regions (see Figure 2 and Table 1 for a summary). The plasma observations show that Juno crossed into the open field line region, but they do not support crossing into a closed field line region. The open field line region was characterized by a very different ion composition to the neighboring plasma disk. The presence of H_2^+ and H_3^+ was detected inside and outside (in wake) of Ganymede's magnetosphere. Low energy (~0.1 to 1 keV) electrons are enhanced just outside the magnetopause: in the wake on the inbound trajectory and in the magnetopause boundary layer on the outbound trajectory.

Acknowledgments

This work was funded by the NASA New Frontiers Program for Juno, at the University of Iowa through contract 699041X, at the University of Colorado through contract 699050X, and at Princeton University through contract NNM06AA75C with the Southwest Research Institute Stefan Duling received funding from the European Research Council under the European Union's Horizon 2020 research and innovation programme (Grant agreement No. 884711).

Open Research

The data presented here resides at NASA's Planetary Data System. The JADE data may be found at https://doi.org/10.17189/1519715. Juno Magnetometer data are at https://doi.org/10.17189/1519711. Text files associated with the figures presented in this paper are accessible at DOI 10.5072/zenodo.1074153.

Captions

Table 1. General plasma properties for the regions delimited in Figure 2.

Figure 1. Geometry of the flyby from Juno in the Ganymede-Phi-Orbital reference frame. The color-coded bands on each side of the track correspond to the count rates for ions with speeds >80 km/s (lower left) or <80km/s (top right) in the spacecraft frame. Low speed ions dominate near Ganymede in the region of partially open field lines. The boundaries "A", "B", …, and "E" are identified in Figure 2 and described in the text. "X" corresponds to closest approach. Outside of region C-D, the magnetic field lines connect to Jupiter. Inside of region C-D, the magnetic field lines connect to Jupiter and Ganymede. The shaded portion of Ganymede is the night side.

Figure 2. (a) TOF counts/s spectrogram, (b) heavy (m/q≥8) and (c) light (m/q=1) ions intensities spectrograms, (d) >0.5 keV H^+ pitch angles, (e) electron intensities and (f) pitch angle spectrograms, (g) electron partial densities and (h) electron energy flux (0.032 to 32 keV) for two pitch angle ranges, and (i) magnetic field magnitude and components (in the Ganymede-Phi-Orbital reference frame). The vertical dashed lines indicate the boundaries between regions of different properties. "MP" stands for magnetopause.

Figure 3. Ion counts/s energy-time spectrograms and energy-per-charge (E/q) versus mass-per-charge (m/q) for two time intervals: top is for plasma disk (before boundary A in Figure 2) and bottom is for Ganymede magnetosphere (between boundaries C and D).

Figure 4. Electron observations: panels (a-b) are energy and pitch angle spectrograms (same as panels (e-f) in Figure 2). Panels (c-g) are average intensities as a function of energy at the times indicated (in the title and with the arrows to panel (a)). The three colored curves correspond to three pitch angle ranges indicated on the right. Panels (h-l) are average intensities as a function of pitch angle at the times indicated. The different colors correspond to different energy ranges indicated on the right.

References

Allegrini, F., Kurth, W. S., Elliott, S. S., Saur, J., Livadiotis, G., Nicolaou, G., Bagenal, F., Bolton, S., Clark, G., Connerney, J. E. P., Ebert, R. W., Gladstone, G. R., Louarn, P., Mauk, B. H., McComas, D. J., Sulaiman, A. H., Szalay, J. R., Valek, P. W., Wilson, R. J. (2021). Electron partial density and temperature over Jupiter's main auroral emission using Juno observations. Journal of Geophysical Research: Space Physics, 126, e2021JA029426. https://doi. org/10.1029/2021JA029426

374 Clark, G., Mauk, B. H., Paranicas, C., Kollmann, P., Haggerty, D., Rymer, A., et al. (2022).
375 Energetic charged particle observations during Juno's close flyby of Ganymede.
376 Geophysical Research Letters, this issue.

377 Connerney, J.E.P., Benn, M., Bjarno, J.B., Denver, T., Espley, J., Jorgensen, J. L., et al. (2017).
378 The Juno Magnetic Field Investigation. *Space Sci. Rev.* 213: 39–138.
379 https://doi.org/10.1007/s11214-017-0334-z

380 Duling, S., Saur, J., Clark, G., Allegrini, F., Greathouse, T., Gladstone, R., et al. (2022).
381 Ganymede MHD model: Magnetospheric context for Juno's PJ34 flyby. Geophysical
382 Research Letters, this issue.

383 Ebert, R. W., Allegrini, F. Angold, N., Bagenal, F., Bolton, S. J., Connerney, J. E. P., et al.
384 (2022). Evidence for magnetic reconnection at Ganymede's upstream magnetopause
385 during the PJ34 Juno flyby. Geophysical Research Letters, this issue.

386 Frank, L. A., Paterson, W. R., Ackerson, K. L., & Bolton, S. J. (1997). Low-energy electron
387 measurements at Ganymede with the Galileo spacecraft: Probes of the magnetic
388 topology. Geophysical Research Letters, 24(17), 2159–2162.
389 https://doi.org/10.1029/97GL01632

390 Greathouse, T., Gladstone, R., Molyneux, P. M., Versteeg, M. H., Hue, V., Kammer, J., et al.
391 (2022). UVS observations of Ganymede's aurora during Juno orbits 34 and 35.
392 Geophysical Research Letters, this issue.

393 Hansen, C., Bolton, S., Sulaiman, A., Duling, S., Brennan, M., Connerney, J., et al. (2022).
394 Juno's close encounter with Ganymede - an overview. Geophysical Research Letters, this
395 issue.

396 Kim, T. K., Ebert, R. W., Valek, P. W., Allegrini, F., McComas, D. J., Bagenal, F., et al. (2019).
397 Method to Derive Ion Properties From Juno JADE Including Abundance Estimates for
398 O^+ and S^{2+}. Journal of Geophysical Research: Space Physics, 125, e2018JA026169.
399 https://doi.org/10.1029/2018JA026169

400 Kim, T. K., Ebert, R. W., Valek, P. W., Allegrini, F., McComas, D. J., Bagenal, F., et al. (2020).
401 Survey of Ion Properties in Jupiter's Plasma Sheet: Juno JADE-I Observations. Journal of
402 Geophysical Research: Space Physics, 125, e2019JA027696. https://doi.org/10.

403 1029/2019JA027696

404 Kivelson, M. G., Bagenal, F., Jia, X., Khurana, K., & Volwerk, M. (2022). "Ganymede : Its
405 Magnetosphere and its Interaction with the Jovian Magnetosphere", in: "Ganymede", eds.
406 M. Volwerk, M. McGrath, X. Jia and T. Spohn, Cambridge University Press, Cambridge,
407 UK, pre-press, 2022.

408 Kurth, W. S., Sulaiman, A. H., Hospodarsky, G. B., Menietti, J.D., Mauk, B. H., Clark, G.,
409 Allegrini, F., Valek, P., Connerney, J. E. P., Waite, J. H., Bolton, S. J., Imai, M.,
410 Santolik, O., Li, W., Duling, S., Saur, J., Louis, C. (2022). Juno Plasma Wave
411 Observations at Ganymede. Geophysical Research Letters, this issue.
412 https://doi.org/10.1029/2022GL098591

413 Mauk, B. H., Haggerty, D. K., Jaskulek, S. E., Schlemm, C. E., Brown, L. E., Cooper, S. A., et
414 al. (2017). The Jupiter Energetic Particle Detector Instrument (JEDI) investigation for the

Juno mission. Space Science Reviews, 213(1–4), 289–346. https://doi.org/10.1007/s11214-013-0025-3

McComas, D. J., Alexander, N., Allegrini, F., Bagenal, F., Beebe, C., Clark, G., et al. (2017). The Jovian auroral distributions experiment (JADE) on the Juno mission to Jupiter. Space Sci. Rev., Volume 213, Issue 1–4, pp. 547–643. doi: 10.1007/s11214-013-9990-9.

Romanelli, N., DiBraccio, G.A., Modolo, R., Connerney, J. E. P., Ebert, R. W., Martos, et al., (2022). Analysis of Juno Magnetometer observations: comparisons with a global hybrid simulation and indications of Ganymede's magnetopause reconnection, Geophysical Research Letters, this issue.

Roth, L., Ivchenko, N., Gladstone, G. R., Saur, J., Grodent, D., Bonfond, B., et al. (2021). A sublimated water atmosphere on Ganymede detected from Hubble Space Telescope observations. *Nature Astronomy*, *5*(10), 1043–1051. https://doi.org/10.1038/s41550-021-01426-9

Saur, J., Duling, S., Wennmacher, A., Willmes, C., Roth, L., Strobel, D. F., et al. (2022). Oscillating north-south brightness ratio of Ganymede's auroral ovals: Hubble Space Telescope observations during Juno's PJ34 flyby. Geophysical Research Letters, this issue.

Szalay, J. R., Smith, H. T., Zirnstein, E. J., McComas, D. J., Begley, L. J., Bagenal, F., Delamere, P. A., Wilson, R. J., Valek, P., Poppe, A. R., Nénon, Q., Allegrini, F., Ebert, R. W., Bolton, S. J. (2022). Water-group pickup ions from a Europa-genic neutrals orbiting Jupiter. Geophysical Research Letters, 49, e2022GL098111. https://doi.org/10.1029/2022GL098111.

Valek. P. W., Waite, J. H., Ebert, R. W., Allegrini, F., Bagenal, F., Szalay, J. R., Wilson, R. (2022). In situ ion composition observations of Ganymede's outflowing ionosphere. Geophysical Research Letters, this issue.

Weber, T. Moore, K., Connerney, J.E.P., Espley, J., DiBraccio, G., Romanelli, N. (2022). Updated spherical harmonic moments of Ganymede from the Juno flyby, Geophysical Research Letters, this issue.

Williams, D. J., Mauk, B. H., McEntire, R. W., Roelof, E. C., Armstrong, T. P., Wilken, B., et al. (1997). Energetic particle signatures at Ganymede: Implications for Ganymede's magnetic field. Geophysical Research Letters, 24(17), 2163–2166.

448
449 **Table 1.** General plasma properties for the regions delimited in Figure 2.
450

	Region	Ions Heavy ions: m/q ≥ 8 Light ions: m/q = 1	Electrons PAD = Pitch Angle Distribution
Jupiter's magnetosphere	before A (16:43:00) after E (17:01:06)	Plasma disk composition (H^+, H_2^+, O^+, S^{2+},O^{2+}, S^{3+}, S^+,O^{3+}) Heavy ions: ~1-20 keV Light ions: ~0.1 – 2 keV Density: Before A: H^+ ~1.1 cm^{-3}, Heavies ~7.9 cm^{-3} After E: H^+ ~1.3 cm^{-3}, Heavies ~8.5 cm^{-3}	Energy distribution: roughly power law with spectral index of ~ −1.3 PAD: ~0.03 to ~5 keV: field-aligned ≳10 keV: pancake Partial density: Before A: ~4 to 6 cm^{-3} (average ~4.7) After E: ~5 to 7 cm^{-3} (average ~6.4)
	A-B 16:43:00 to 16:45:08	Plasma disk composition Heavy ions ~1-20 keV Light ions ~0.1 – 2 keV	Energy distribution: ≲1 keV enhanced PAD: similar to before A but with a clear depletion near 90° at all energies Partial density: ~3 to 8 cm^{-3} (average ~5.2)
Wake	B-C 16:45:08 to 16:49:48	Heated distribution Plasma disk composition and H_3^+ Density: H^+ ~0.7 to 2.3 cm^{-3} (average ~1.6) Heavies ~5.7 to 24 cm^{-3} (average ~15)	Energy distribution Heated ≲1 keV enhanced, peak at ~0.4 keV PAD: ~uniform based on partial coverage from JADE Partial density: ~3.3 to 20 cm^{-3} (average ~9)
Ganymede's magnetosphere	C-D 16:49:48 to 17:00:39	Mixed composition Slow, cold distributions (strong spin modulation of ~30 s), speed <80 km/s: Ganymede magnetosphere (H^+,H_2^+, H_3^+, O^+,O_2^+, and maybe OH^+ and H_2O^+) Plasma disk, speed >80 km/s (similar to A-B & B-C) PAD: Precipitating field-aligned H^+ and empty upward loss cone Slower ions flowing away from Ganymede	Energy distribution: roughly power law with spectral index of ~ −1.45 bump at ~1 keV PAD (from ~16:55): 0.03 to ~5 keV: uniform with depleted upward loss cone ≳10 keV: slightly depleted downward loss cone (near closest approach) and depleted upward loss cone
Magnetopause	D-E 17:00:39 to 17:01:06	Plasma disk composition (similar to A-B & B-C)	Energy distribution: ≲3 keV enhanced, peak at ~0.4 keV PAD: Similar to before A but with enhancement near 90° for ~0.4 to 6 keV Possible electron conic at 17:01:03-04 Partial density: ~3.4 to 12 cm^{-3} (average ~7)

451
452
453

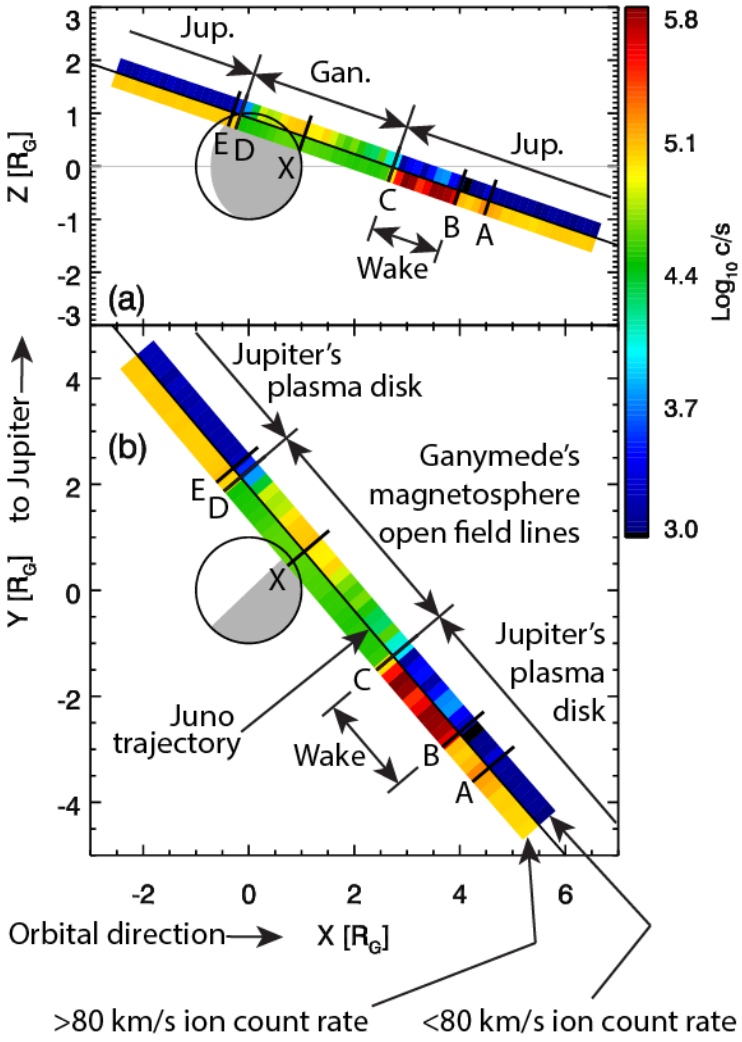

Figure 1. Geometry of the flyby from Juno in the Ganymede-Phi-Orbital reference frame. The color-coded bands on each side of the track correspond to the count rates for ions with speeds >80 km/s (lower left) or <80km/s (top right) in the spacecraft frame. Low speed ions dominate near Ganymede in the region of partially open field lines. The boundaries "A", "B", …, and "E" are identified in Figure 2 and described in the text. "X" corresponds to closest approach. Outside of region C-D, the magnetic field lines connect to Jupiter. Inside of region C-D, the magnetic field lines connect to Jupiter and Ganymede. The shaded portion of Ganymede is the night side.

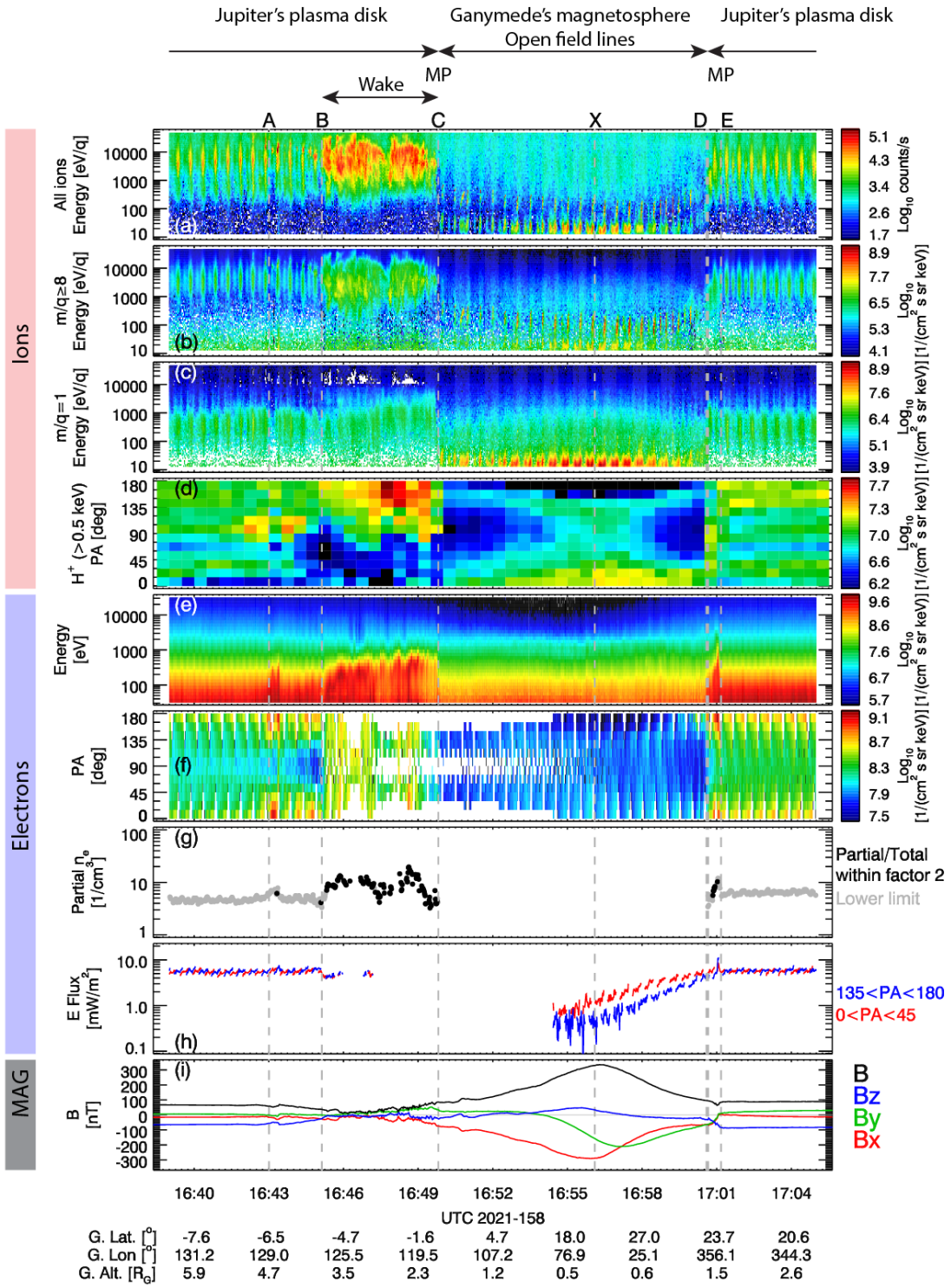

Figure 2. (a) TOF counts/s spectrogram, (b) heavy (m/q≥8) and (c) light (m/q=1) ions intensities spectrograms, (d) >0.5 keV H^+ pitch angles, (e) electron intensities and (f) pitch angle spectrograms, (g) electron partial densities and (h) electron energy flux (0.032 to 32 keV) for two pitch angle ranges, and (i) magnetic field magnitude and components (in the Ganymede-Phi-Orbital reference frame). The vertical dashed lines indicate the boundaries between regions of different properties. "MP" stands for magnetopause.

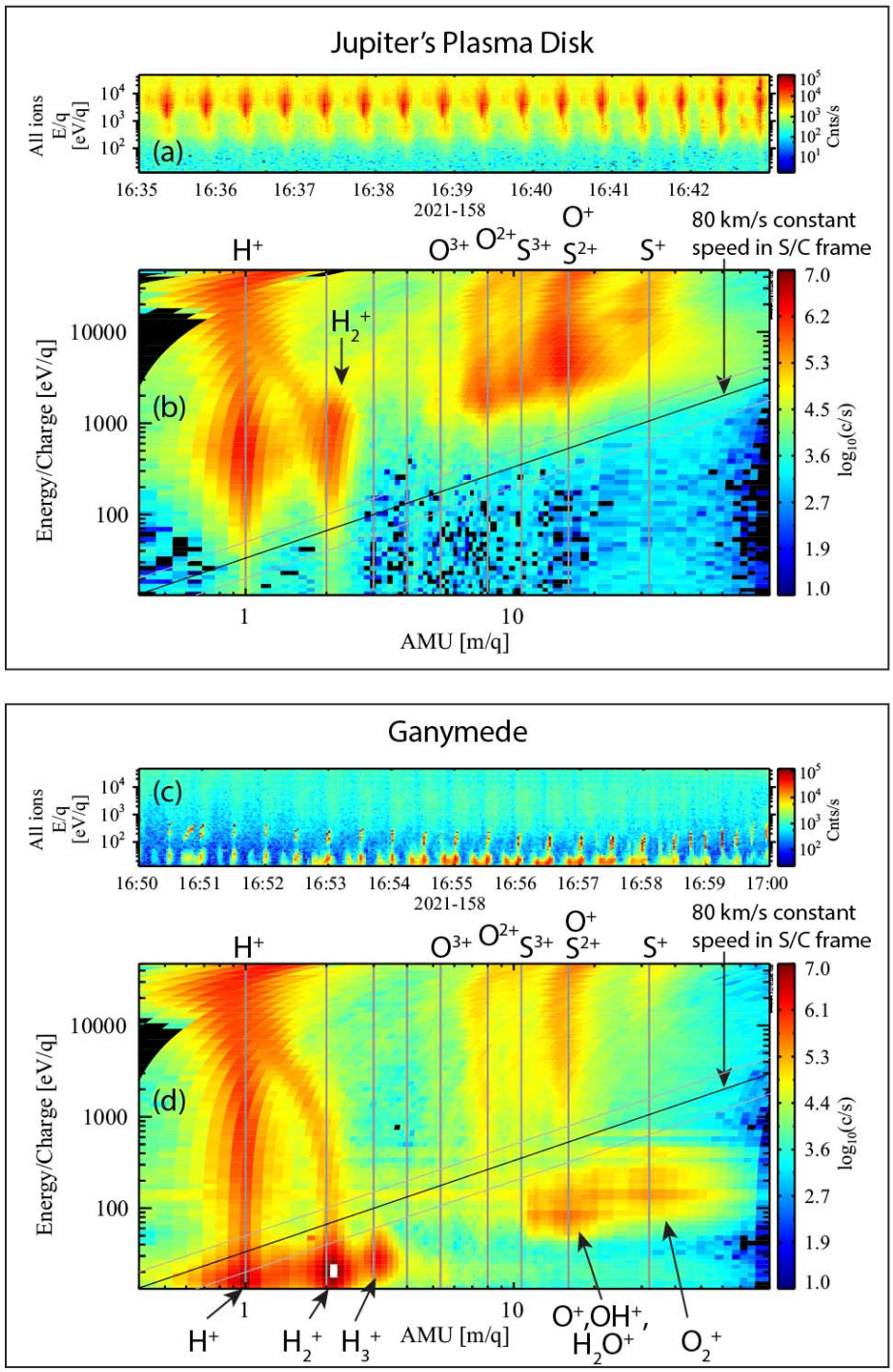

Figure 3. Ion counts/s energy-time spectrograms and energy-per-charge (E/q) versus mass-per-charge (m/q) for two time intervals: top is for plasma disk (before boundary A in Figure 2) and bottom is for Ganymede magnetosphere (between boundaries C and D).

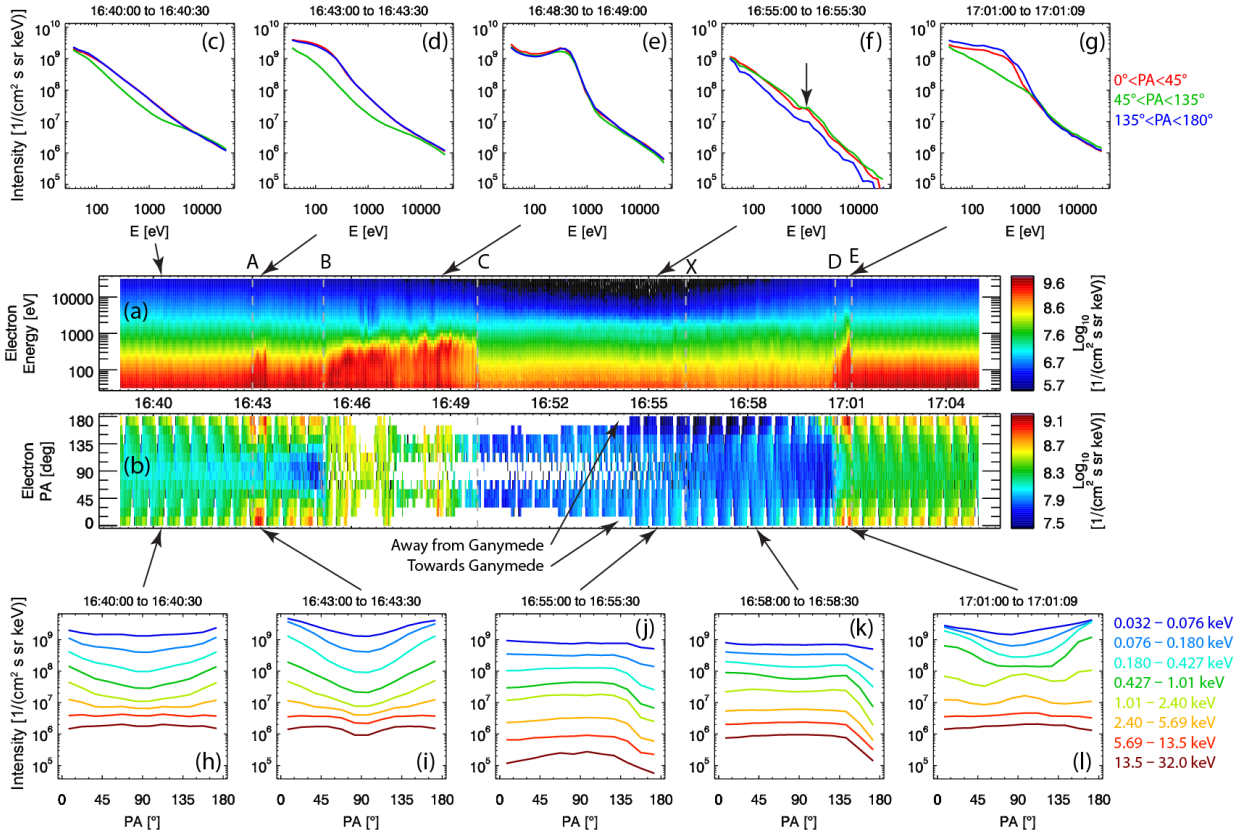

Figure 4. Electron observations: panels (a-b) are energy and pitch angle spectrograms (same as panels (e-f) in Figure 2). Panels (c-g) are average intensities as a function of energy at the times indicated (in the title and with the arrows to panel (a)). The three colored curves correspond to three pitch angle ranges indicated on the right. Panels (h-l) are average intensities as a function of pitch angle at the times indicated. The different colors correspond to different energy ranges indicated on the right.

Figure 1.

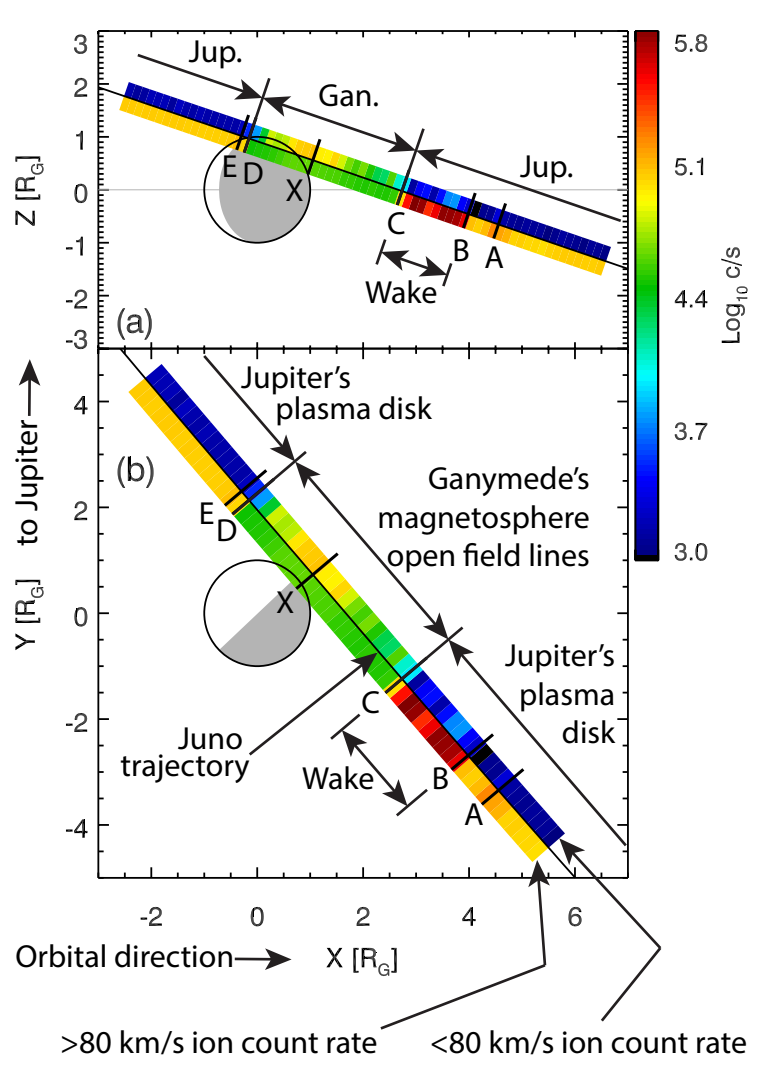
Jup.
Gan.
Jup.
E
D
X
C
B
A
Wake
(a)
Z [R_G]
Log10 c/s
5.8
5.1
4.4
3.7
3.0
Jupiter's plasma disk
(b)
Ganymede's magnetosphere open field lines
Jupiter's plasma disk
Juno trajectory
Wake
to Jupiter
Y [R_G]
Orbital direction
X [R_G]
>80 km/s ion count rate
<80 km/s ion count rate

Figure 2.

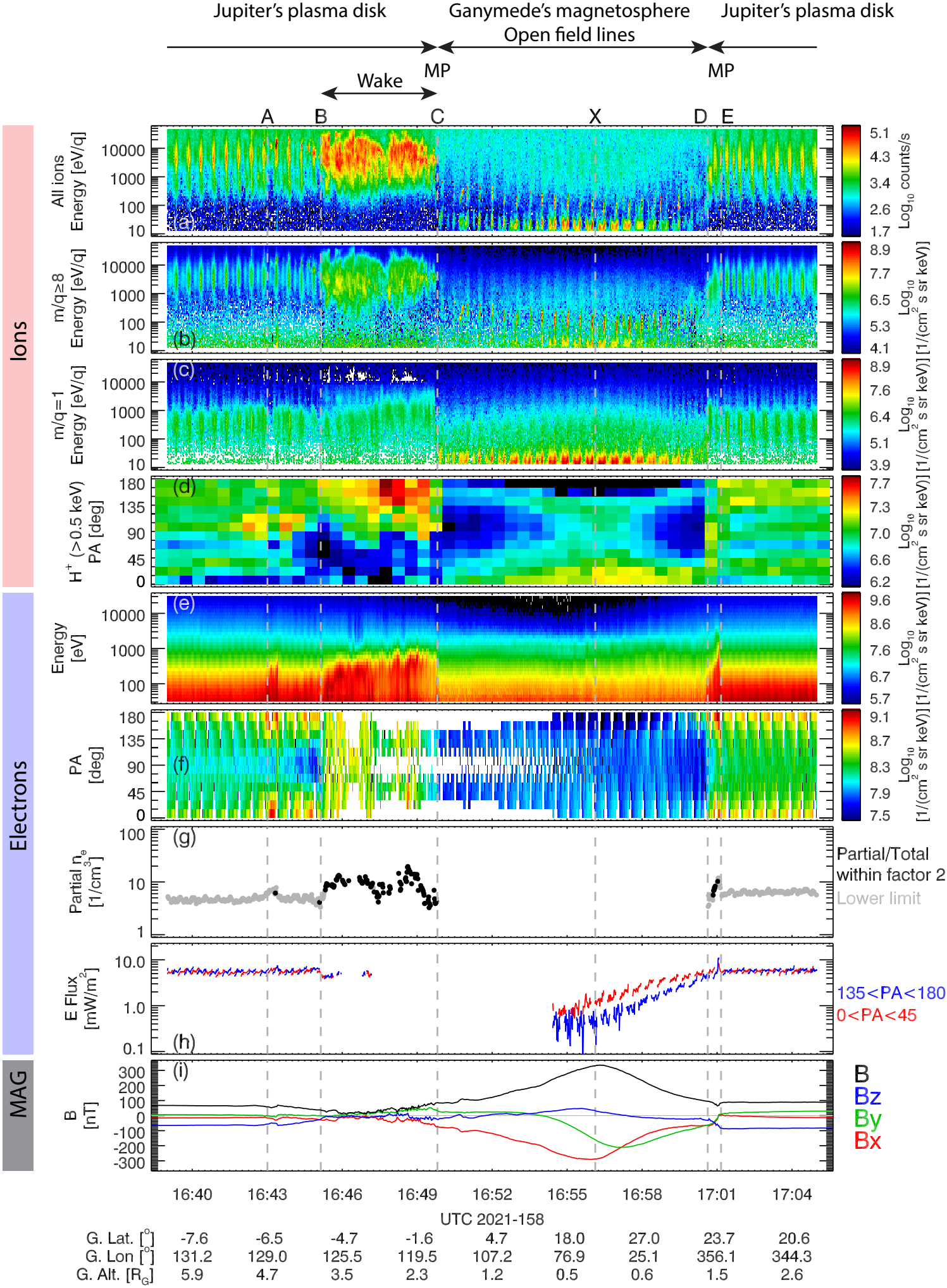
Jupiter's plasma disk
Ganymede's magnetosphere
Open field lines
Jupiter's plasma disk
MP
MP
Wake
A
B
C
X
D
E
Ions
Electrons
MAG
All ions Energy [eV/q]
m/q≥8 Energy [eV/q]
m/q=1 Energy [eV/q]
H+ (>0.5 keV) PA [deg]
Energy [eV]
PA [deg]
Partial ne [1/cm3]
E Flux [mW/m2]
B [nT]
Log10 counts/s
Log10 [1/(cm2 s sr keV)]
Partial/Total within factor 2
Lower limit
135<PA<180
0<PA<45
B
Bz
By
Bx
16:40
16:43
16:46
16:49
16:52
16:55
16:58
17:01
17:04
UTC 2021-158
G. Lat. [°] -7.6 -6.5 -4.7 -1.6 4.7 18.0 27.0 23.7 20.6
G. Lon [°] 131.2 129.0 125.5 119.5 107.2 76.9 25.1 356.1 344.3
G. Alt. [RG] 5.9 4.7 3.5 2.3 1.2 0.5 0.6 1.5 2.6

Figure 3.

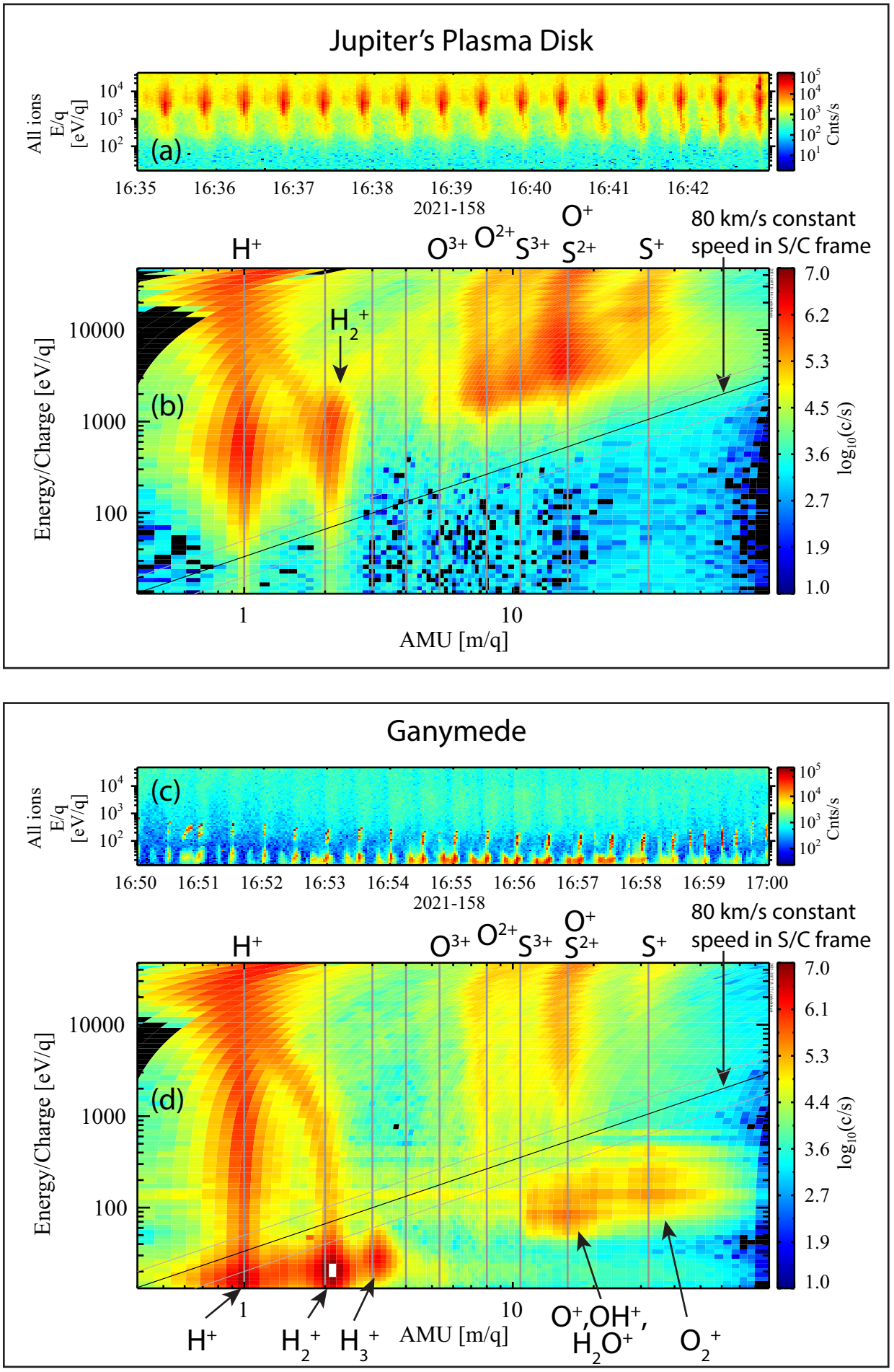
Jupiter's Plasma Disk
All ions E/q [eV/q]
(a)
Cnts/s
16:35
16:36
16:37
16:38
16:39
16:40
16:41
16:42
2021-158
H+
O3+
O2+
S3+
O+
S2+
S+
80 km/s constant speed in S/C frame
H2+
(b)
Energy/Charge [eV/q]
log10(c/s)
AMU [m/q]
Ganymede
(c)
16:50
16:51
16:52
16:53
16:54
16:55
16:56
16:57
16:58
16:59
17:00
(d)
H+
H2+
H3+
O+,OH+, H2O+
O2+

Figure 4.

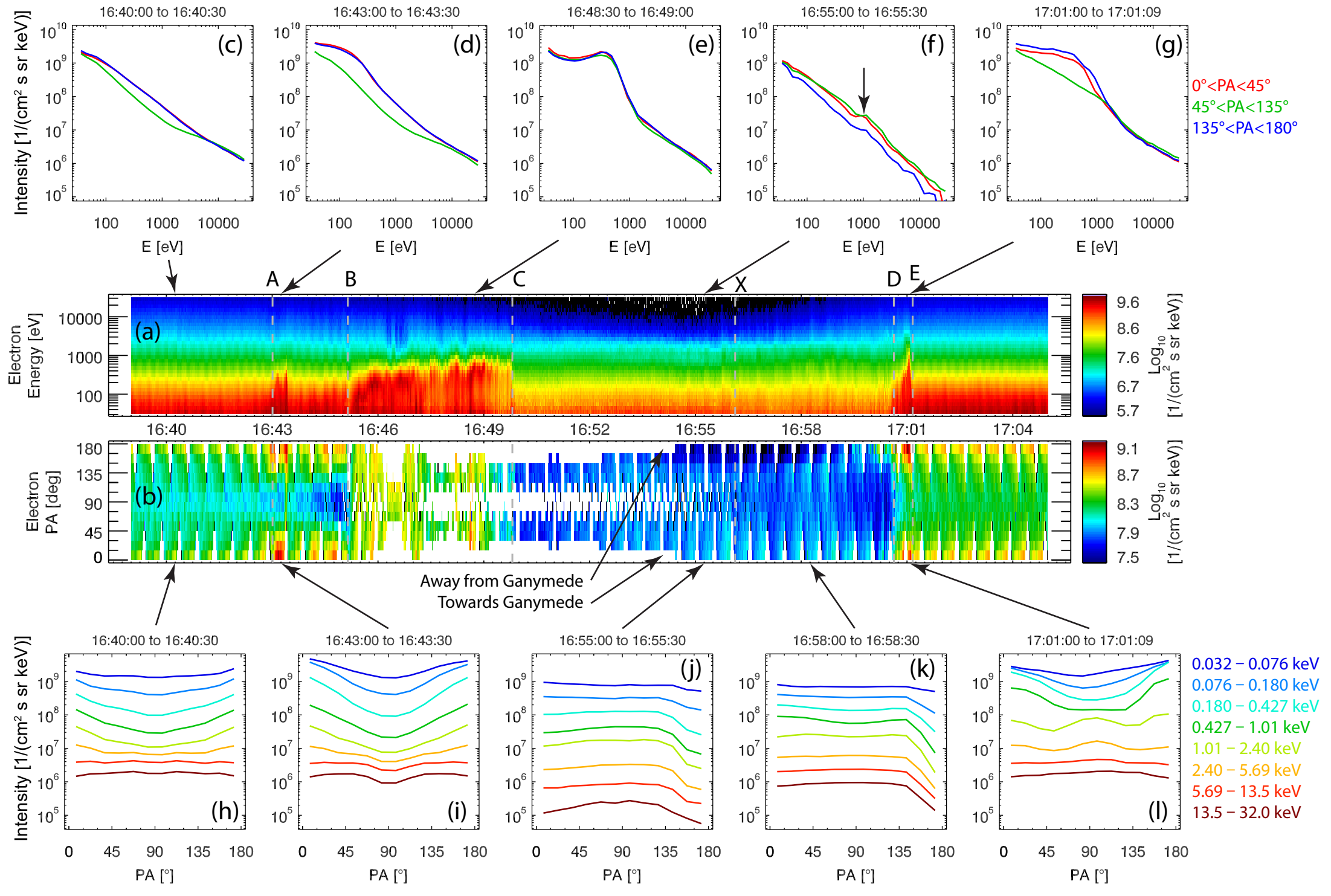
16:40:00 to 16:40:30
16:43:00 to 16:43:30
16:48:30 to 16:49:00
16:55:00 to 16:55:30
17:01:00 to 17:01:09
(c)
(d)
(e)
(f)
(g)
Intensity [1/(cm² s sr keV)]
E [eV]
0°<PA<45°
45°<PA<135°
135°<PA<180°
A
B
C
X
D
E
(a)
Electron Energy [eV]
Log10 [1/(cm² s sr keV)]
16:40
16:43
16:46
16:49
16:52
16:55
16:58
17:01
17:04
(b)
Electron PA [deg]
Away from Ganymede
Towards Ganymede
16:40:00 to 16:40:30
16:43:00 to 16:43:30
16:55:00 to 16:55:30
16:58:00 to 16:58:30
17:01:00 to 17:01:09
(h)
(i)
(j)
(k)
(l)
PA [°]
0.032 – 0.076 keV
0.076 – 0.180 keV
0.180 – 0.427 keV
0.427 – 1.01 keV
1.01 – 2.40 keV
2.40 – 5.69 keV
5.69 – 13.5 keV
13.5 – 32.0 keV